THE 1962 FLASH FLOOD IN THE RUBÍ STREAM (BARCELONA, SPAIN)

J.P. Martín-Vide[(1)], M.C. Llasat[(2,3)]

[(1)] Technical University of Catalonia – BarcelonaTech, Barcelona, Spain.

[(2)] Department of Applied Physics, University of Barcelona, Barcelona, Spain

[(3)] Institute of Water Research (IdRA), University of Barcelona, Barcelona, Spain

Corresponding author: Juan P. Martín-Vide. Technical University of Catalonia – BarcelonaTech. c/ Jordi Girona 1-3, D1, 08034 Barcelona

ABSTRACT

The 1962 Rubí flood was a severe flash flood, the worst to ever take place in Spain, claiming the lives of more than 800 people following 200 mm of rainfall in 2 hours. Such a high number of casualties can be explained by the very high vulnerability of people who lived in the floodplains of a wandering, ephemeral stream (a wadi) prone to flash floods. Many publications to commemorate the 50th anniversary of the flood have been used as proxy data for the event, especially in terms of social aspects. The meteorological and pluviometric information is reviewed, while other information is only found in grey literature. Recently, the event has been considered an outlier in the panorama of European flash floods. Because of the above, this paper aims to convey all the information to readers and show that it deserves to be raised to an international level as an example of an extreme flash flood. After addressing some misunderstandings, it can be concluded that the event was not an outlier, nor was it extreme, in terms of total rainfall, return period, discharge, discharge per unit basin area, unit stream power and flow velocity. It may be extraordinary

because the flood reached very high levels by transporting large amounts of both fine and coarse sediment particles. The stream is steep, ephemeral, lacking an armour layer, and prone to torrential events, in which the large sediment transport played a role in how high the flood levels rose. The use of flooding marks to compute discharges is also discussed. In addition, the paper presents a torrential calculation based on the momentum principle in a control volume.

1. Introduction

Flash floods in Catalonia are not exceptional. They usually occur in summer and early autumn, and are favoured by low level instability and high temperatures in the Mediterranean Sea. Summer events are often local flash floods in small, torrential, ephemeral streams (wadis). They are mostly located in coastal areas where the population is more densely-concentrated (Llasat et al., 2014), which means vulnerability and exposure is at its highest. An example is the flash flood event recorded on 31 July 2002 on the central coast of Catalonia with more than 200 mm in less than 24 hours and damages of about € 9.7 million. Autumn flood events, in turn, are a consequence of more organized disturbances, usually caused by the presence of a surface or deep low pressure (Llasat, 2009). In spite of the decisive role played by the Mediterranean Sea in these cases, the impact of the Atlantic is not negligible, providing the necessary water vapour to sustain the process in the middle and high troposphere. In this sense, the role of atmospheric rivers from the Atlantic is now a subject of study in reconstructions of the most remarkable historical flood events (Ramos et al., 2015). The floods and flash floods that took place between 6 and 9 November 1982 in Catalonia, Aragon, and southeast France, with maximum daily precipitation values above 500 mm, illustrate these kinds of events (Gibergans-Bàguena and Llasat, 2007; Trapero et al., 2013). This seasonal distribution is common in the northwest Mediterranean region, where the “flood season” is mainly concentrated from August to November (Llasat et al., 2013).

From 1900 to 2011, 277 flood events, mainly flash floods, were recorded in Catalonia, and 61 of these events caused catastrophic damage (Llasat et al., 2016). Regarding the western county of

Vallés, which includes the Rubí stream basin close to Barcelona, and which was critically hit by the September1962 flash flood, the number of events for the 1900-2015 period was 53. Although less catastrophic than September 1962, another flash flood occurred in the same basin (Rubí) two months later, which worsened the structural damages of the September flood. In spite of later events in September 1971 (Llasat et al., 2007), October 1987 (Ramis et al,1994) and June 2000 (Llasat et al., 2003; Amengual et al., 2007), this flash flood event of 25 September 1962 remains the most important event recorded in Spain in the 20th century. No exact data on damages and deaths are available, except what was published in the newspaper La Vanguardia (the most important newspaper at the time) on 28 September: 441 people dead, 374 missing, 213 seriously injured and losses of around 2650 millions of pesetas (which would be 533 million euros in 2013).

Regarding the geomorphic changes brought about by flash floods, the particular case of small, ephemeral, Mediterranean rivers should be highlighted. Shifts in channel position, river bank erosion and impacts on longitudinal stream profiles are the main changes that can be expected (Conesa-García, 1995). Manmade changes in these kinds of streams, such as stream channelization or river profile controls through bed sills (Martín-Vide and Andreatta, 2009) hinder both channel shifts and bank erosion, leaving bed profile changes (vertical) as the only adjustment in the long term. The 1962 flash flood event in the Rubí stream occurred before any significant manmade changes had developed.

Gaume et al., (2009), in their compilation of European flash floods since 1946, reported the exceptional case of the September 1962 flash flood in the Rubí stream to the international community. It was exceptional because of the number of deaths in Terrassa and Rubí, the two cities the stream passed through, which reached over 450, the highest in their data set, in addition to the huge damages. However, the event appeared as an outlier in terms of its peak discharge for the small catchment area, and so it was excluded from the data set (Gaume et al., 2009). This paper is devoted to revisiting the data for this flood, for which there is only some knowledge on a national level. Although data is limited, hopefully we will show that the flood deserves to be

79 considered on an international level as an example of an extreme flash flood, instead of a dubious
80 outlier, with the sediment load properly taken into account.

81 The data for the 1962 flood are revisited in the following paragraphs from a meteorological,
82 pluviometric, hydraulic, hydrological and sediment transport point of view. The aim of the paper
83 is to prove that the peak discharge values deserve to be considered seriously (not discarded as
84 though the estimates were inaccurate). The paper starts by describing the Rubí creek and the flash
85 flood event.

86

87 2. Study area and its socioeconomic characteristics in 1962

88 The Rubí creek is a torrential ephemeral stream in the Llobregat river basin (total surface area of
89 4,948 km^2), passing through the cities of Terrassa and Rubí (Fig.1 and Fig. 2), separated by 10
90 km along the river path. The main tributary, called Les Arenes, drains an upper basin (highest
91 peak of 1104 m) covered with Mediterranean forest, and then spreads out from the mouth of the
92 valley into an alluvial fan. In this lower part, the stream over the fan is a very wide, steep (≈ 3%
93 gradient), wandering channel that crosses the eastern outskirts of the first city, Terrassa. The
94 average annual rainfall over the basin is approximately 650 mm, but the flow regime is strongly
95 ephemeral —just two or three times per year. The catchment area is 30 km^2 at the junction with
96 its smaller western tributary, which drains a mostly urban basin where most of the city stands
97 (Fig.2). After the junction of the two tributaries, the main Rubí creek crosses the centre of the
98 second city (Rubí) where the catchment area is 82.4 km^2 (Martín-Vide et al., 1999). There, the
99 profile is not so steep (≈ 1% gradient) and the flow regime is intermittent.

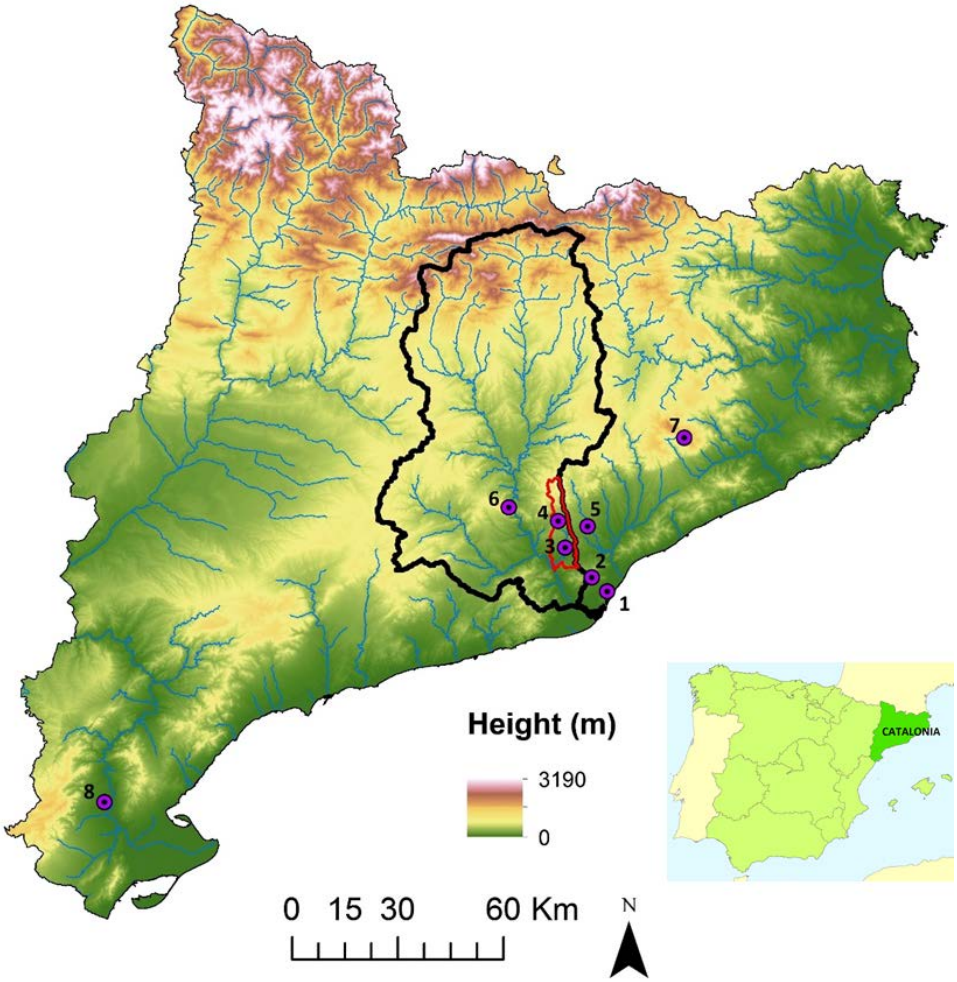

Figure 1. Digital Terrain Model of Catalonia showing the Llobregat basin, the Rubí basin (red) and the cities, towns and observatories cited in the paper: 1) Barcelona, 2) Fabra Observatory, 3) Rubí, 4) Terrassa, 5) Sabadell, 6) Montserrat, 7) Montseny, 8) Tortosa (DTM provided by the Institut Cartogràfic i Geològic de Catalunya, ICGC).

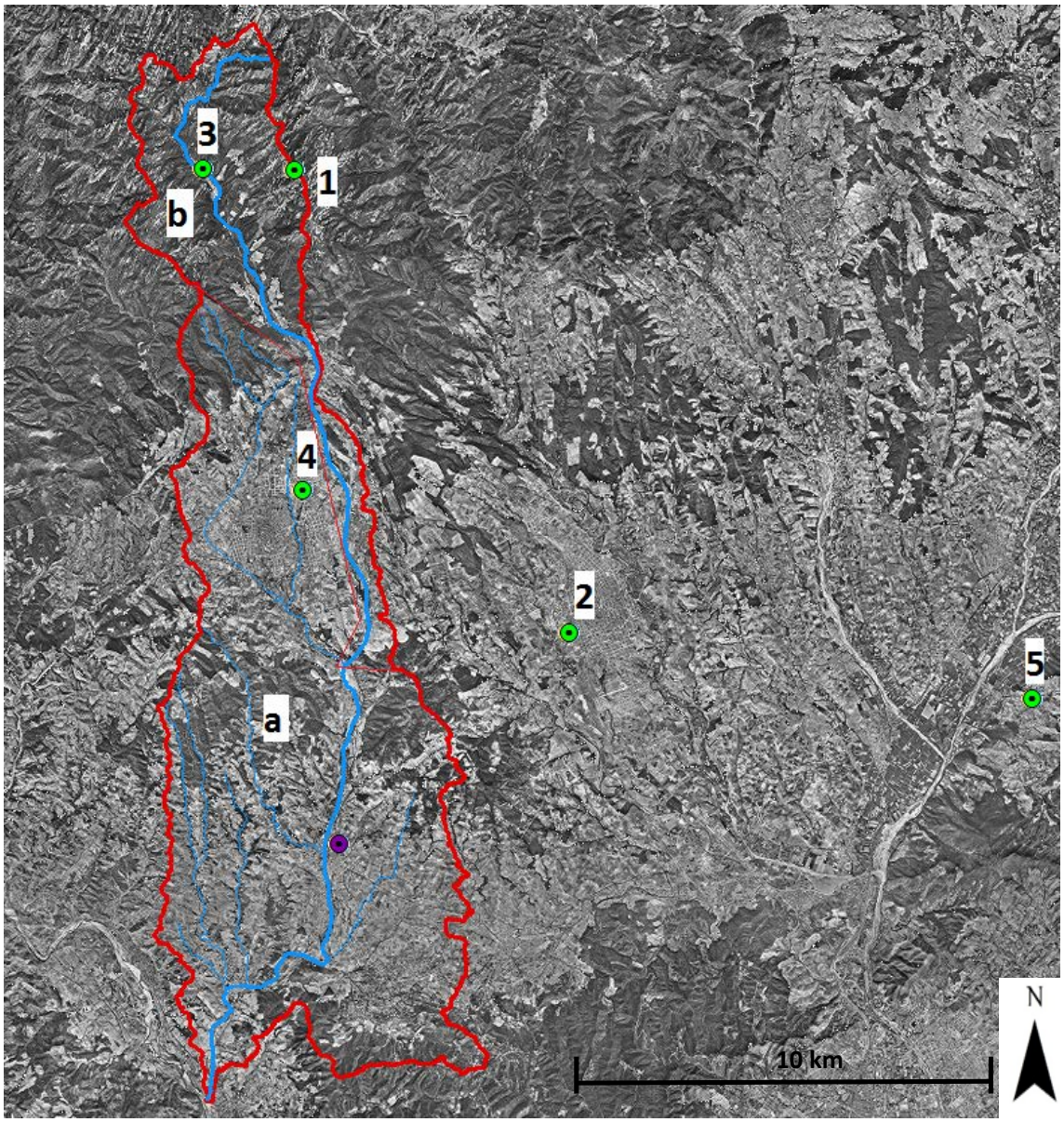

Figure 2. Rubí basin (red contour); the border between the upper basin and its western tributary is drawn in a thin red line. At their junction the stream changes its name, from Les Arenes upstream (b) to Rubí downstream (a). Rainfall gauges (see Table 1): 1) Sant Llorenç del Munt, 2) Sabadell, 3) Matadepera, 4) Terrassa, 5) Martorelles. The town of Rubí is shown in purple (from a 1956 ortophoto at a 1:5000 scale, provided by ICGC)

The sediment yield is high, due to the particular basin geology. The basin is dominated by conglomerates of deltaic origin from the Eocene-Oligocene, with thick inserts of sandstone, loam and loess. Conglomerate cobbles are mainly formed of limestone and quartz from Palaeozoic slate. Conglomerate cement is dominated by clay. The resistance to erosion is low, especially

between strata. Fines from loess and the conglomerate matrix are largely available to detachment by overland flow and gully development and, secondly, the extensive conglomerate rock cover is easily weathered, releasing rounded clasts of all sizes. The bed of the tributary is very flat, wide and well sorted with a median size of D_{50} = 15 mm, in the range of medium gravel, and a mean size of D_m = 50 mm (Martín-Vide et al., 1999). A thorough campaign carried out just after a moderate flood demonstrated the non-layering of this gravel bed, i.e. the lack of a surface or an armouring layer coarser than the material underneath, which typically occurs in ephemeral streams (García and Martín-Vide, 2001). The features of highly available fines and clasts, and of no armouring in the bed, allow for transport of both a high wash load and a high bed material load.

In 1962, the industries in the flooded cities produced more than 90% of the total textile market in Spain (Valls i Vila, 2012). Migration to these cities was continuous at that time; families came from less-developed regions of Spain every day (in 1945 the population of Terrassa was 51,000, and by 1965, it was 118,000). Entire neighbourhoods and industries were placed on the riverbed or on floodplains of the ephemeral streams (see Fig. 3). The housing problem was dealt with by constructing new legal housing, yet in many cases this housing was located in a flood prone area. Cheap houses and shacks were built in high-risk flood areas, and some apartments were rented out to so many people that they took turns to sleep in the house. In addition to this significant human exposure, some constructions and factories added extra vulnerability. There was a lack of structural prevention measures. Flood risk awareness was almost nil, notably among the migrant population who were unfamiliar with flash floods. The preparedness level was very low due to a lack of Civil Protection or any organized emergency management whatsoever. The lack of forecasting tools and methodologies at that time, and the difficulties in the communication chain (radio was the most common media), are additional factors.

3. The 1962 flash-flood event in the Rubí stream

On the night of 25 September 1962, a storm delivered a large amount of rainfall in a few hours, leaving behind the devastated urban landscape shown in Figure 3 the next morning in the outskirts

of the first city. The aspect of the strean in the aftermath is that of a wadi after a flood. The flow went overbank of its wide, cohesionless, alluvial channel, probably because of some avulsion and also of diversion by the blocking of the bridge in the background of the photo taken by a plane (Fig. 3a). This meant the channel resumed its shifting over the alluvial fan. Traces of the flood are visible in the new channel bed on the right, opened that night over traces of an old channel. They are even more visible in the sharp cut made by this channel through the neighbourhood. People were gathering in front of the remaining houses, standing over the new bed that was the high ground the evening before (Fig. 3a). The new channel also flanked the right of the railway bridge just downstream. The bridge itself was swept away, except for the rails left hanging in place (Fig. 3b). Riverbank erosion and the scour of the channel supplied bed material to the stream downstream. The devastated area in the photograph is 22 hectares and over 100 people died there. Geomorphic changes that took place were the shift in channel position and extensive riverbank erosion.

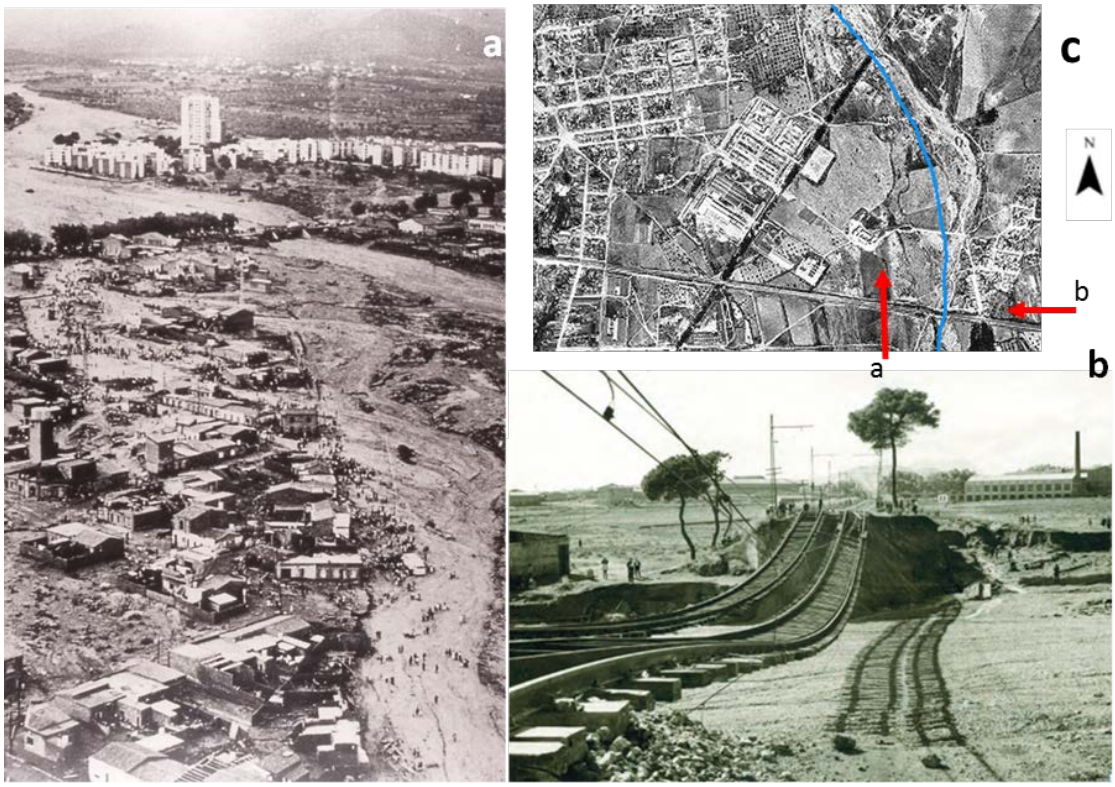

Figure 3 a) View from a plane of the Les Arenes wadi looking upstream, 26 September 1962. The coordinates measured from the source of the creek are x=13.2 km for the bridge in the

158 background of the photo and x≈14.0 km for the stream channel in the foreground; b) Railway
159 bridge over Les Arenes, situated just after the downstream edge of the aerial photo (a); c) aerial
160 photograph dated 1956, six years before the catastrophe; the arrows point to the location of
161 photos (a) and (b); note the quick house building from 1956 (c) -1962 (a); the blue line is the
162 modern stream channel (channelized).

163 Regarding the centre of the second city, Rubí, the houses and factories had encroached on the
164 stream channel in the years prior to 1962. The weakest were torn down by the flood. The scale of
165 the devastation is illustrated with real data in Figure 4 and photographs in Figure 5. Note the
166 extremely high flow elevation, much higher than a bridge that was swept away that night. Note
167 also the area of the buildings torn down within the flooded area. The impression in the aftermath
168 is not that of a clean cut new channel in an alluvial plain anymore, but a razed industrial and living
169 quarter, dirtied with sediment and debris. There were no significant geomorphic changes. The
170 devastated urban area of Rubí shown in Figure 4 was around 3 hectares, and the death toll there
171 was similar to the first city, Terrassa (Fig. 3).

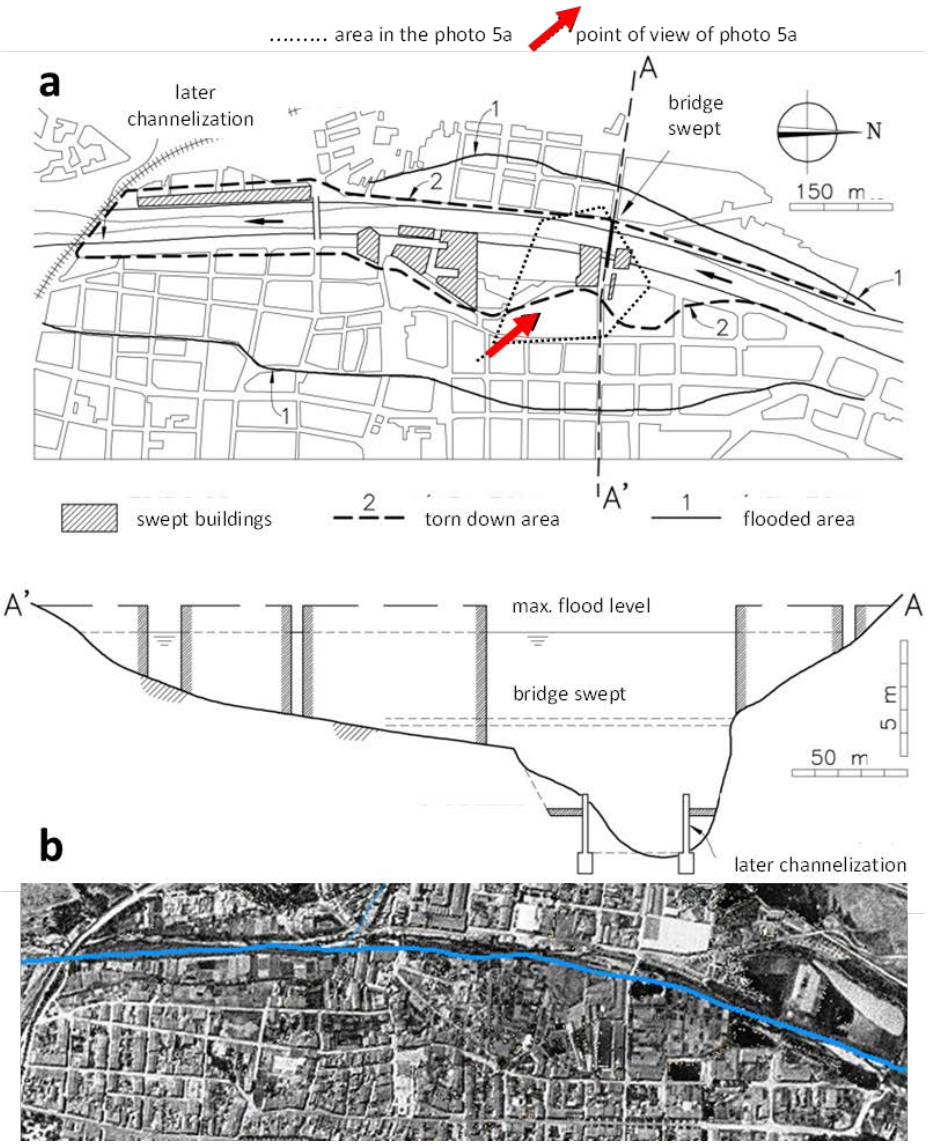

172

173 Figure 4 a) Plan and cross section A-A´ of Rubí town, with details of the 1962 flood level. The
174 urban reach in the plan goes from coordinate x=22.4, measured from the source, upstream, to
175 x=23.7 km downstream. Modified from Martín-Vide (2006); b) aerial photograph dated 1956;
176 note the stream encroachment in 1962 (a); the blue line is the modern channelized path.

177 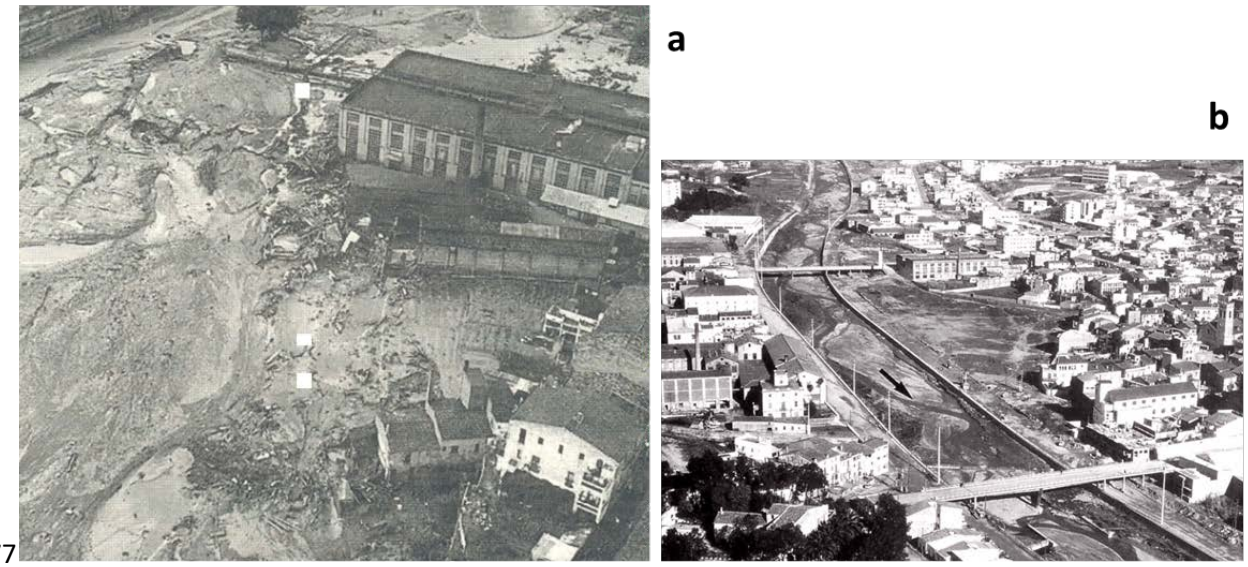

178 Figure 5 a) Photograph from a plane of Rubí, 26 September 1962. b) The same photo a couple
179 of years later with the channelization in the same area. Picture **a** shows a close-up of picture **b**
180 (see the big factory in both photos on the left floodplain). The point of view of (5a) is shown in
181 Figure 4.

182 Rescue teams had difficulty accessing some areas due to the height reached by the flow and the
183 power cuts caused by the thunderstorm. Numerous homes, bridges as well as part of the road and
184 rail network were completely destroyed. Almost 80% of the damage was inflicted to industry and
185 commercial sectors: for example, 50 textile factories and more than 200 homes and 80 cars were
186 damaged in Sabadell (see Fig.1 for situation). Crops were lost and many vineyards were uprooted
187 by the flow. More than 4.000 people were left homeless and many others lost their jobs. The
188 indirect socioeconomic damage was incalculable. Indeed, production was interrupted for several
189 weeks in most factories, for months in others, or they were even closed permanently. Besides, the
190 majority of the financial aid granted by the state to recover regular activity never reached end
191 users. The incoming migratory flux to this region became an outgoing flux after the flood event,
192 as a consequence of the loss of relatives, jobs and homes (Valls i Vila, 2012).

193 For most of the data for the 1962 flash flood, we are indebted to the work of López Bustos et al.
194 (1964). An author among them, Coll Ortega (1963), published some of the same data before.
195 These reports are grey literature, unfortunately in terms of the international awareness of the Rubí

196 flash flood. These engineers carried out a survey after the flood, identifying flood marks, drawing
197 cross sections and providing, after calculations, some impressive figures about sediment transport.
198 They introduced the notion of 'virtual' as opposed to 'real' flow discharges. 'Virtual' refers to the
199 discharge calculated at the surveyed cross sections with a reasonable bed roughness coefficient.
200 The virtual discharge was always much higher than the discharge inferred from the basin
201 hydrology under the input of real rainfall, which was called the 'real' discharge. They attributed
202 the difference between the virtual and real discharge to the effect of a huge sediment load, both
203 in terms of wash load and bed material load, which increased the actual equivalent roughness
204 much higher than mere bed friction under clear water. In doing so, they followed the theory of
205 'flow with debris' published at the time by the engineer García Nájera (1943, 1962), which today
206 is classified as the flow of a Newtonian fluid carrying a high suspension and bedload (Mintegui,
207 1993), herein called torrential flow from now on. The water depths and velocities of this torrential
208 flow can be solved by a so-called torrential method, that will be described and applied (in an
209 updated version) in the Section 4.4.

210 A contemporary to López et al., (1964), Pardé (1964), in a book of more general interest, made
211 estimates of the rainfall and peak discharge, which implicitly are 'real' discharges because they
212 are related to precipitation. He also stressed the amount of mud and pebbles in the flow, and
213 pointed out that some narrow bridges failed to release water and sediment, with peak discharges
214 of 1000—1200 m^3/s that had an impact on several kilometres of the stream.

215 These publications from 1963-1964 are mentioned before the data review in the next section, in
216 order to show the response of the scientific community at the time. The use of the epochal terms
217 'virtual' and 'real' may be misleading because: firstly, the very real event reached the marks used
218 to calculate the virtual discharge; and secondly, the 'virtual' discharge greatly overestimates the
219 real discharge, which seems to run counter to the usual meaning of the two words. Finally, the
220 real discharge is actually derived from sparse measurements of rainfall, not from any flow
221 measurement, through runoff estimations and hydrological modelling, as we will see later. The

terms ‘apparent’ or ‘field-based’ and ‘rainfall-based’ will be used in preference to ‘virtual’ and ‘real’, respectively.

4. Data available for the 1962 flood

4.1. Main meteorological and pluviometric features

The meteorological situation was an anticyclone in surface over west Europe and the Mediterranean Sea (Fig. 6a), which allowed the accumulation of water vapour in the low levels of the troposphere, favoured by the very warm days prior to the event (28ºC in Barcelona and 30ºC in south Catalonia on 24 September). Instability was increased by the strong warm advection from the south in the low and middle levels (Fig. 6b). At upper levels a trough placed at the northwest Iberian Peninsula, associated with a cold front, explained the precipitation in other parts of Spain and the relative cold air over Catalonia (Fig. 6c). All these factors joined to high Convective Available Potential Energy (CAPE) cumulating in the west of the Mediterranean due to the high previous temperatures. This great convective instability was probably triggered by the Littoral mountain chain. The wind analysis in surface pressure (Fig. 6d) points to a mesoscale low in front of the Catalan coast, following a typical mesoscale configuration associated with heavy rainfall in Catalonia, as was the case on 10 June 2000 (Llasat et al., 2003; Rigo and Llasat, 2005). While not clear in synoptic charts, this is confirmed by the decrease in sea level pressure measured in several meteorological stations; as an example, pressure fell from 1016 hPa on 24 September at 07:00, to 1009 hPa on 25 September at the same time.

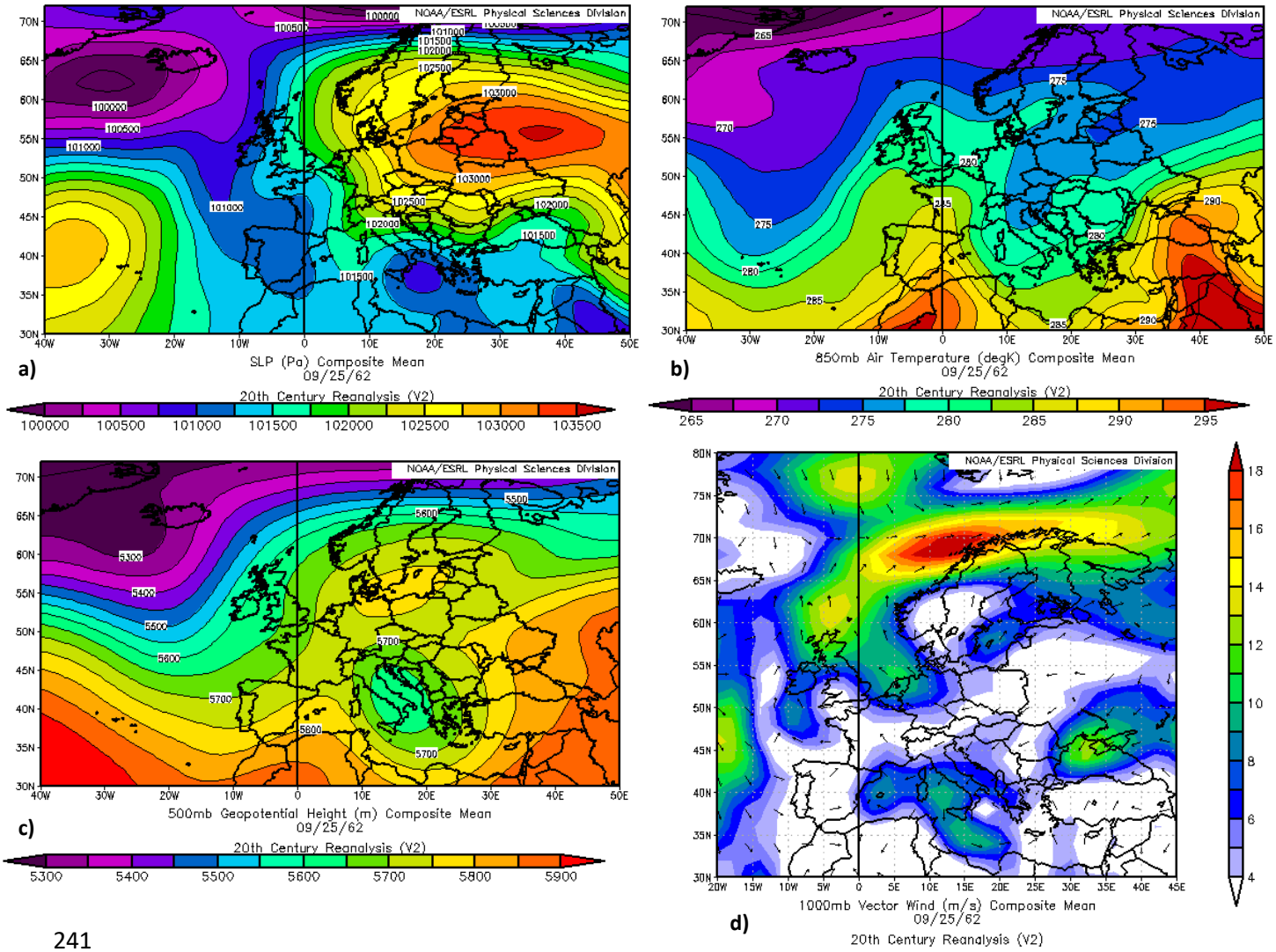

241

242 Fig. 6 a) Mean sea level pressure on 25 September 1962 (source: NOAA), b) Mean temperature
243 at 850 hPa on 25 September 1962 (source: NOAA), c) Mean geopotential height at 500 hPa on
244 25 September 1962 (source: NOAA), d) Composite mean on wind at 1000 hPa on 25 September
245 1962 (source: NOAA)

246 The only image taken by the meteorological satellite TIROS that day was sent by the US Army
247 to the National Meteorological Service of Spain (Martín León, 2012). This image confirms the
248 passage of a cold front over the Iberian Peninsula, and the presence of a deep convection over
249 Catalonia, probably associated to multi-cellular systems. Qualitative observations in surface
250 reported a sky covered by stratiform clouds on the day, with growing cumulonimbus clouds in
251 the afternoon and evening (Llasat, 1987).

252 Many publications to commemorate the 50th anniversary of the disaster have been used as a proxy
253 data for more details about the event dynamics (Valls i Vila, 2012; Aulet et al., 2012). The storm
254 started on the afternoon of 25 September. Following the Ebro Observatory (Tortosa, Fig. 1), a
255 squall line crossed the southeast of the region between 15:30 and 17:00 local time (14:30 and
256 16:00 UTC), although lightning was observed all day long. Thunderstorm activity is proven by
257 records from the main observatories in Catalonia at that time. At 17:30 local time, drivers had to
258 switch on their car lights on the roads because it turned dark, as if it were night. At 18:00 local
259 time, the Montserrat mountain (Fig.1) was buried under the clouds. Around the same time, traffic
260 on some roads was interrupted due to heavy rainfall. A witness said it was like an iron curtain.

261 With no weather radar at the time, the proxy data point to a strongly convective event, following
262 the definition initially presented in Llasat (2001) and updated in Llasat et al. (2016). This means
263 that more than 80% of the rainfall exceeds the intensity threshold of 1 mm/min for 1-min series,
264 and more than 6 mm/min at some point. Indeed, a pluviograph in Sabadell recorded 135.8 mm,
265 with a maximum intensity of 6 mm/min at 21:51, 95 mm between 21:38 and 22:19 (average
266 intensity of 2.3 mm/min) and more than 100 mm between 21:30 and 22:27 local time on 25
267 September 1962, when it stopped raining. This pluviograph was the same type of recording gauge
268 as the one used by the Fabra Observatory (Barcelona), with the longest rainfall rate series in the
269 world (starting in 1921) used for research on convective precipitation (Llasat, 2001; Puigcerver
270 et al. 1986). This observatory and the Montseny observatories (Fig.1) recorded a maximum
271 rainfall rate at 23:50 local time (22:50 UTC), measuring 144 mm/h and 100 mm/h, respectively.
272 A lack of common criteria for the time, whether local or UTC, may have a bearing on
273 incoherencies. Witnesses in the basin said the most intense rain fell between 21:00 and 23:00
274 local time (Valls i Vila, 2012). Pardé (1964) wrote that the rainfall in the basin was around 150-
275 175 mm in a period of 2-3 hours.

276 The rainfall map in Figure 7a was built on the basis of original handwritten daily forms. At that
277 time, the records between 18:00 of the day D and 18:00 GMT of day D+1 were assigned to day
278 D. The map was drawn by hand with this in mind, so that it covers the storm on the night of 25

September and the following morning (Llasat, 1987). Rainfall was concentrated on a strip of land along a mountain range and its hillsides and plains, not far from the sea. The uplands of Rubí creek (1104 masl) belong to that range, yet the maximum daily precipitation was 250 mm east of Rubí (in Martorelles, a flatter area, see also Fig. 2). There must have been a stationary convective system over that strip of land to explain such concentrated rainfall. Figure 7b maps the total rainfall on 25 September (from 7:00 of day D to 7:00 of day D+1, present criterion) by applying an inverse distance weighting (IDW) interpolation to the data, including a recent database (2016) and over a larger domain. The Rubí basin draining to the two cities falls fully under the isohyets 180-200 mm, yet areas west and east of Rubí are under the 220-250 mm range. However, the catastrophe only occurred in Rubí.

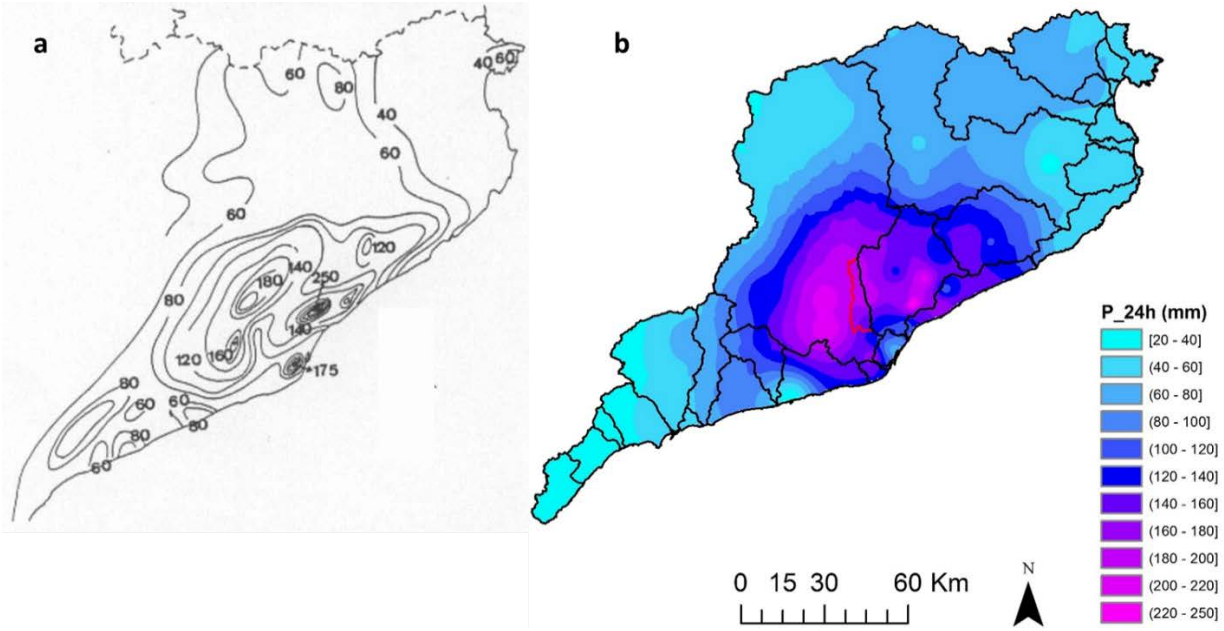

Figure 7 a) Map of the total precipitation recorded between 18:00 on 25 September and 18:00 on 26 September 1962, according to the original records at the AEMET archives in Barcelona (source: Llasat, 1987). b) Map of the total precipitation recorded between 07:00 on 25 September and 07:00 on 26 September 1962, including data from the current AEMET database after an IDW interpolation; the domain covered is Catalonia, except for the basins draining to the Ebro river. The Rubí basin is shown in red contour (compare with Fig.1).

Finally, Table 1 shows the daily precipitation recorded in the Rubí basin and its surroundings, together with the total precipitation between 24 and 26 September 1962 according to the official data, which shows a maximum cumulated rainfall of 360 mm in Martorelles.

	St Llorenç del Munt (1)	Sabadell (2)	Matadepera (3)	Terrassa (4)*	Martorelles (5)
25 Sept	182 mm	135.8 mm	200 mm	223 mm	250 mm
26 Sept	11 mm	2.6 mm	0 mm	0 mm	110 mm

Table 1. Precipitation recorded on 25 and 26 September 1962. Data have been previously submitted to manual quality control, taking into account the original files, the official 2016 AEMET database and eyewitness accounts. *according to Coll Ortega (1963). See Fig. 2 for gauge location.

For the sake of comparison, the daily point rainfall in the basin for return period of 10, 100 and 500 years are 125, 185 and 225 mm, respectively. These numbers come from the isohyets maps published for the whole country by the Public Works Department in 1999. Therefore, the 1962 storm would match 100 years in gauge (1), 500 years in gauge (4) and a figure in between in gauge (3), with all three gauges within the Rubí basin (Table 1). Altogether, the return period most cited in grey literature on the 1962 flood is 200 years.

4.2. Hydraulic data

López et al. (1964) surveyed two cross-sections, S1 and S2, in their fieldwork. They were located around four kilometres upstream of the bridge in the background of Figure 3a (upstream of Terrassa). They surveyed two more cross-sections a shorter distance upstream of the urban borders of Rubí (Fig. 4), S3 and S4. The four are redrawn in Figure 8, and their exact positions are shown later in Figure 9. A specific report about cross-section S2 is given by Coll Ortega (1963). Another similar data is cross-section A-A´, taken at the bridge swept away by the flood in Figures 4 and 5. This does not come from López et al. (1964), but from an archival search (Martín-Vide, 2006).

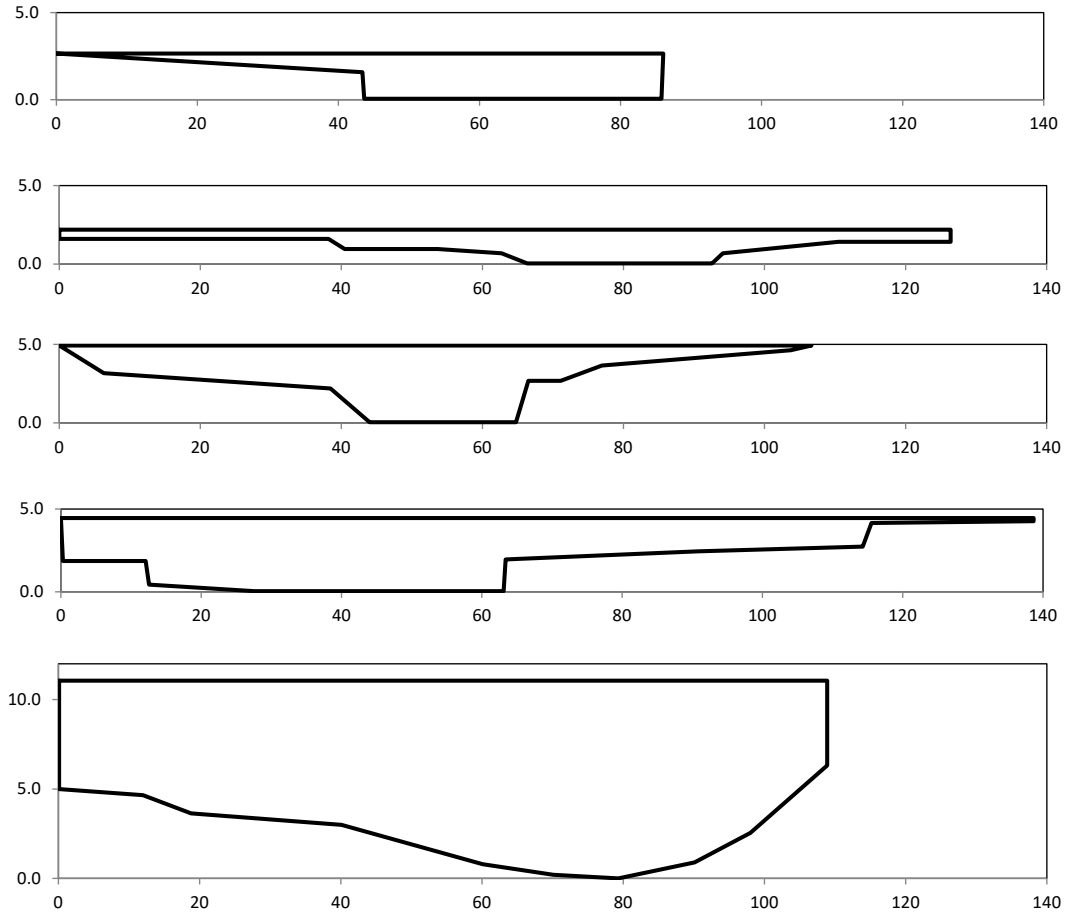

Figure 8. From top to bottom, cross sections S1, S2, S3 and S4, taken from the report drawn up after the flood (López et al., 1964 and Coll-Ortega, 1963). Distances and elevations in m. Corresponding depths, widths and flow areas are given in Table 2. The fifth cross-section is A-A´ in Figure 4, located at x≈22.8 km, where x is the coordinate measured from the source. In A-A´ only the span between the two nearest buildings to the left and right of the main channel (Fig.4) is taken into account.

By using the surveyed cross-sections and bed gradients, López et al. (1964) calculated field-based discharges with the Bazin equation (Table 2). Very similar results can be obtained today with the more commonly-used Manning formula, with a roughness coefficient in the range of n= 0.026—0.030, which makes sense for the coarse beds of that kind in torrential ephemeral streams. In fact, by using the Strickler formula for grain roughness with D_m =50 mm (see above), n=0.029. Some other figures that are useful for this discussion are included in Table 2: specific discharge per unit basin area, excess shear stress on the bed, and unit stream power.

	x km	A km^2	S_0 1962 %	H m	W m	flow area m^2	R_h m	virtual Q m^3/s	real Q m^3/s	ratio -	unit (real) Q $m^3/s/km^2$	virtual v m/s	real v m/s	excess shear θ/θ_c (-)	unit (real) stream power (Wm^{-2})
S1	9.4	22	3.25	2.6	86	134	1.49	1130(2)	320	3.5	14.5	8.43	2.39	12.5	1185
S2	10.3	24	2.94	2.2	126	157	1.23	1390	350	4.0	14.6	8.85	2.23	9.3	800
S3	20.7	57	1.19(1)	4.9	107	248	2.28	1680	635	2.6	11.1	6.77	2.56	7.0	695
S4	22.5	82	1.50(1)	4.4	139	365	2.53	3130(2)	658	4.8	8.0	8.58	1.80	9.8	695

Table 2. Basic data for cross-sections S1 to S4 (Figure 8, except for A-A´), under the flash flood of 1962 according to López et al. (1964) and Coll Ortega (1963). x is the abscissa from the source along the bed profile (see Fig. 9), A is the drainage area, S_0 is the bed slope, H is the water depth, W is the width, R_h is the hydraulic radius, Q is the discharge, 'ratio' is the ratio of field-based ('virtual' in the heading) over rainfall-based ('real' in the heading) magnitudes, either Q or v, and v is velocity. The other columns are added for discussion purposes. (1)These data are a little discordant with each other and with respect to Figure 9, shown later. (2)These data were not given by López et al. (1964), but have been recalculated using their method (they used the Bazin formula, which reads $C = 87/(1+k/R_h^{½})$, where C is the Chézy coefficient and k is equal to 1.55, equivalent to a Manning roughness coefficient in the range of 0.026—0.030). Unit Q refers to the specific discharge per unit basin area, the stream power is $9800 \cdot (Q('real')/W) \cdot S_0$ and the excess shear is $\theta = R_h \cdot S_0 / 1.65 \cdot D_m$ (dimensionless shear stress on the bed) and $\theta_c = 0.047$, following the Meyer-Peter and Müller formula (critical θ).

Regarding the fifth cross-section in Figure 8, section A-A´, close to S4, the depth attained was 10.5 m, 2.4 times more than depth in S4. Meanwhile the flow area was 935 m^2, 2.6 times larger than in S4, and the apparent discharge would be 13,900 m^3/s, 4.4 times higher than in the S4 cross-section and over 20 times higher than the rainfall-based discharge there. This point is key for our discussion.

Apart from the open channel flow itself, the hydraulic structures may have played a role during the event. In 1962 there were no river training structures in place, and more specifically there was

356 no channelization wall (those shown in Fig. 5b were built later). Thus, the flow was able to widen
357 the channel by eroding its banks, a process shown in Figure 3a. This mechanism fed the flow
358 downstream with sediment. However, there were several bridges. Bridges were prone to be
359 clogged by log and boulders carried by the flood, as witnesses have consistently mentioned (see
360 Fig. 3a). Moreover, three bridges failed that night: 1) the railway bridge shown in Figure 3b; 2) a
361 bridge that spanned the main tributary very close to the junction, and 3) the bridge swept away in
362 central Rubí, shown in Figures 4 and 5a. Eyewitnesses, once again, gave accounts of the roaring
363 large waves or surges that rolled down that night, probably due to bridge failures. Interestingly,
364 cross-sections S1 and S2 are located well upstream of the collapsed bridges, while cross-sections
365 S3 and S4 are downstream of the first two collapsed bridges, and section A-A´ was measured
366 right at the third one (see Fig. 9).

367 4.3. Hydrological data

368 This section comes after the hydraulic data because the apparent discharges were the main focus
369 in López et al. (1964). The authors estimated rainfall-based peak discharges, as well. In retrospect,
370 we think they used a kind of *reductio ad absurdum* reasoning to evaluate the peak discharges: if
371 the apparent discharges had been the real flow rate, that is to say if the flood marks had been the
372 effect of a pure water flow, then the runoff coefficient would have fallen within the range
373 0.8—1.1, which means that the runoff volume would have been larger than the rainfall volume
374 (i.e. a runoff coefficient >1). The authors final estimate of rainfall-based discharges is given on
375 Table 2. Consequently, the ratio of apparent, field-based over rainfall-based discharge was larger
376 or much larger than 2, according to their calculations. The same ratio applies to velocities, with
377 the apparent figure over the rainfall-based figure. For Pardé (1964), peak discharges might have
378 attained 400—600 m^3/s for basin areas of 20-25 km^2 (such as S1 and S2) and 700—800 m^3/s for
379 areas about 40-50 km^2. López et al. (1964) estimates were below those made by Pardé.

380 The rainfall and flow discharge were measured in the main tributary (Les Arenes) over the course
381 of 6 years (Martín-Vide et al., 1999). Several heavy rainfall events were recorded, with rainfall
382 of 85 mm in 1 hour and 150 mm in 12 hours, as well as peak discharges of up to 140 m^3/s. The

runoff coefficient was calculated using real data in 8 events, resulting a maximum coefficient of 0.15 and an average of 0.09. One reason for such low figures is the transmission losses over the very wide, flat, pervious bed on the ephemeral main tributary. Although the runoff coefficient can be expected to be higher in an exceptional flood (following, for example, the well-known Soil Conservation Service method), these values provide a context, if not a confirmation, of the relatively low rainfall-based discharges in 1962. We will come back to this point in the discussion.

4.4. Sediment transport data and reanalysis

No real data on sediment transport is available in López Bustos et al. (1964). They merely applied the torrential method mentioned above to cross-sections S1 and S3. They drew the conclusion that the water plus the fine suspended load had a relative density in the range of 1.15—1.20, while the bed material load transport had taken up some 38% in volume of the flowing mass. In other words, the mass was made up of 62% mud (density 1.20) and 38% of solid particles from the riverbed. The impressive figure here is the 38% of bed particles in the volume, which in principle brings about a hyperconcentrated flow. On the other hand, the 1.20 relative density does not fall in this domain, but in the domain of water flood (Costa, 1988).

The large sediment transport allowed López et al. (1964) to explain how a relatively low discharge swelled up to reach such high flood marks (and therefore introducing the apparent discharge). An order of magnitude for the real bedload transport in the tributary has been provided by a sediment trap in the abovementioned research, which was carried out over 6 years (Martín-Vide et al., 1999). The rates of bedload in real events were found to be four times higher than predicted by the Meyer-Peter and Müller (MPM) equation. The measured total volume of bed sediment transported in these events was in the range of 0.7—1.2% of the total runoff volume (Martín-Vide, 2006).

We have updated the theory to apply the same method used by López et al. The underlying concept is the torrential flow, i.e. a flow carrying so much fine and coarse sediment that the velocity is lower and, consequently, the depth is higher than the corresponding so-called ‘clear water’ flow, free of sediment (Meunier, 1991). Apart from flash floods, gravel-bed rivers and

410 ephemeral rivers, the literature on this topic draws from several fields: mountain rivers and steep
411 channels (Rickenmann, 2012), mudflow dynamics (Coussot, 1997; Chen and Wan, 1999),
412 bedload influence on flow resistance (Recking et al., 2008), and even hyperconcentrated flow and
413 debris flow (Wan and Wang, 1994, Takahashi, 2007), among other fields. While not all can be
414 detailed here, some relevant facts are as follows: first, a 1.20 relative density flow carries roughly
415 three times more bedload than the corresponding clear water (Rickenmann, 1991), due to the
416 increase in buoyancy of the particles. In turn, the higher bedload rate should imply a higher flow
417 resistance and so a higher depth (Song et al., 1998, Recking et al., 2008). One reason is that the
418 particles entrained from the bed move more slowly than the water around them (Ashida and
419 Michiue, 1972).

420 In order to apply the method to cross-sections S1 to S4, the longitudinal bed profile (Fig. 9)
421 provides the bed slope, a key factor in bedload transport. Figure 9 is the oldest known bed profile
422 that covers the two cities and the four cross-sections. It dates back to 1973. The less complete
423 1962 bed profile is the highest known profile. In the period 1962-1973, before the data shown in
424 Figures 3-5, the bed profile remained stable in the main tributary while it underwent a parallel
425 degradation in the Rubí stream (Martín-Vide and Andreatta, 2009). Therefore, the 1973 bed
426 slopes are valid for 1962. Indeed, data on the bed slope in Table 2 compares relatively well with
427 Figure 4.

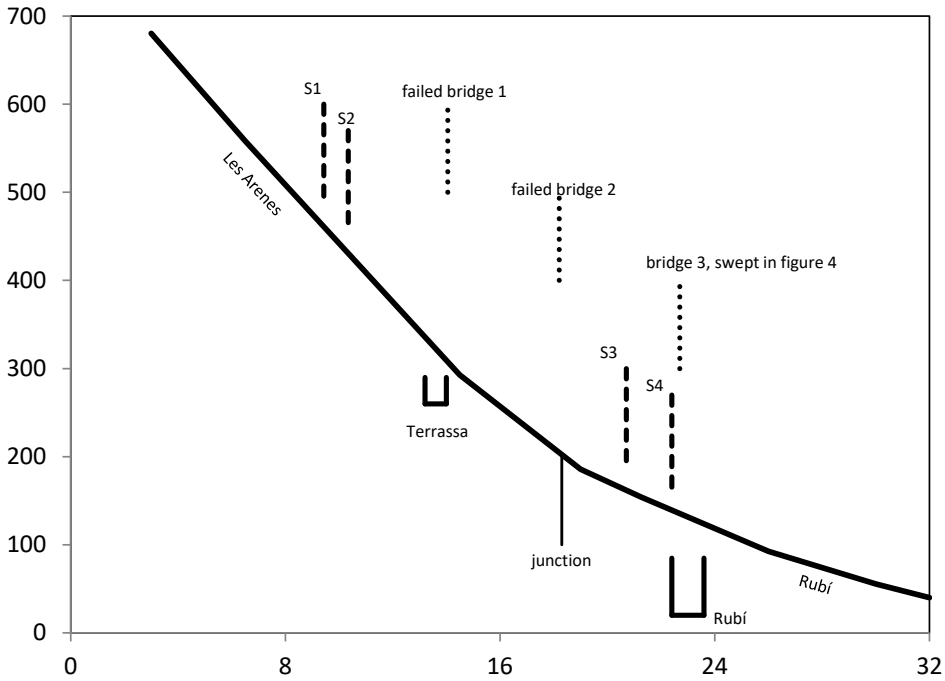

428

x coord (km)	3—6.5	6.5—14.5	14.5—18.3	19—21	21.2—26	26—30	30—32
slope (%)	3.48	3.32	2.37	1.41	1.29	0.92	0.79

429

430 Figure 9. Bed profile of the main tributary and Rubí stream in 1973 (data in the attached table).
431 Abscissas in km, ordinates in m. Note the cross-section positions S1 to S4, the location of the
432 failed bridges and the urban reaches of the cities (Terrassa and Rubí) shown in Figures 3 to 5.

433 The results of the method are presented in Table 3. Densities of 1.20/1.15 have been applied to
434 the upper/lower pair of cross-sections, i.e. to S1-S2 / S3-S4, respectively. The Manning formula
435 is used for clear water, with n=0.030—0.026 respectively for the upper/lower sections. Then, a
436 depth and a velocity of the dense flow (called `mud´ for the sake of brevity) are calculated via
437 mass conservation of water and water with sediment. After that, the MPM formula multiplied by
438 4, according to Martín-Vide et al. (1999), and with the `mud´ flow variables (density, shear stress)
439 provides the bedload Q_s. Finally, the Ashida and Michiue (1972) expression for particle velocity
440 is used:

441 $$v_s = u\,(1 - (\theta/\theta_c)^{-1/2}) \qquad (1)$$

where v_s is the particle velocity, u is the flow velocity and θ/θ_c is the excess shear shown in the caption of Table 2. The magnitudes u and θ are, again, those of the dense flow (`mud´). The torrential method calls for all these magnitudes of clear water flow, `mud´ flow, bedload rate and particle velocity to obtain the maximum torrential depth and velocity by applying the momentum equation to a control volume.

The target of the calculation is the depth recorded by López et al. (Table 2), now called torrential depth in the sense of bulk flow depth. For cross-section S1, for example, the first row in Table 3 shows that a flow of 370 m^3/s, a little higher than the rainfall-based flow in Table 2, is required to hit the target of 2.6 m. On the way to this target, the clear water depth of 370 m^3/s is y_{cl} = 1.60 m, and the `mud´ depth y_m = 1.90, i.e. an increase of 19%. A further 37% depth increase to get to 2.60 m is due to the 7.7% bedload concentration in the flow (Q_s/Q) calculated with MPM × 4, and also to the fact that particles are dragged at a velocity of v_s = 4.72 m/s, according to equation (1), less than the torrential velocity v_t= 4.93 m/s. Note that higher bedload rates, such as the 38% reported in López et al. (1964), are not warranted by the method (then, the flow is not hyperconcentrated). On the way to the target, the clear water velocity v_{cl} (7.54 m/s) is higher than the `mud´ velocity v_m (6.28 m/s) and this, in turn, is higher than the torrential velocity of the mixture v_t , which drags the particles at a lower velocity v_s.

	Q (m^3/s)	relative density (-)	Q_s/Q (%)	cl. water depth H_{cl} (m)	`mud´ depth H_m(m)	torr. depth H_t (m)	target (m)	depth increase %	cl.water v_{cl} (m/s)	`mud´ v_m (m/s)	torr. v_t (m/s)	particle v_s(m/s)	cl. water Fr (-)	torr. Fr (-)
S1	**370**	1.20	7.7	1.60	1.90	2.60	2.6	19—37	7.54	6.28	4.93	4.72	1.90	0.98
S2	**391**	1.20	5.0	1.62	1.76	2.20	2.2	8—25	4.37	3.64	3.03	2.26	1.10	0.65
S3	635	1.15	1.8	3.83	4.04	**4.58**	4.9	5—13	5.17	4.50	4.01	2.55	0.84	0.60
S4	658	1.15	2.3	2.58	2.78	**3.09**	4.4	8—11	5.39	4.69	4.31	2.78	1.07	0.78

Table 3. Results of the torrential method. The bold numbers point to the deviations from the target in S3-S4, and from the rainfall-based discharge in S1-S2 according to López et al (1964) (compare against columns for Q and H in Table 2). $Fr = v_{( )}/(g \cdot H_{( )})^{½}$ is the Froude number,

463 where ( ) stands either for *cl* clear water or *t* torrential flow. The figures of depth increase refer
464 to the shift from clear water to `mud´ flow — and from `mud´ to torrential flow.

465

466 The results are similar for S2, with a required flow slightly higher than in Table 2. However, the
467 target cannot be reached in the other pair of cross-sections. For example, in S4 the flow of 658
468 m^3/s (Table 2) only accounts for a torrential depth of 3.09 m, far from the target of 4.40 m. Neither
469 deviations from this discharge, as applied in S1 and S2, nor deviations from the relative density,
470 manage to raise the depth sufficiently. Namely, the discharge that pushes 3.09 m up to 4.40 m
471 with the same method would be 1760 m^3/s (not shown in Table 3), and this would occur by
472 increasing similar percentages by 8—11% (`mud´—bedload for S4) —a much higher clear water
473 depth. With regard to S3, the distance to the target (4.90 m) is closer, which means that a discharge
474 of 854 m^3/s, closer to Q in Table 2 (not shown in Table 3), would raise the depth up to the target.

475 It is worth pointing out that the results in Table 3 are driven to a large extent by the bed slope. In
476 fact, if the data by López et al. (1964) in Table 2 were replaced by the 1973 bed profile (Fig. 9)
477 in a sensitivity test for the slope, the new gradients at the S3 and S4 cross-sections would result
478 in torrential depths farther from the target for S3, and closer to the target for S4.

479

480 6. Discussion

481 The Rubí basin was not the most severely hit by the storm of 25 September 1962 in terms of total
482 rainfall (Fig.7). However, it was the most vulnerable. Its new migrant population had been pushed
483 to build their homes in flood-prone areas, or within shifting ephemeral streams, unaware of the
484 danger. This is not a new discovery by any means, but the Rubí case study may be a good example
485 of what determines risk. Hundreds of deaths occurred in the two cities through which the Rubí
486 stream passes, while the same cannot be said for other basins. Regarding the technical issues of
487 the flood, discussion is divided in four parts: peak discharge, sediment load, torrential flow and
488 the effect of bridges. A draft of a sensitivity analysis is presented at the end.

489 6.1. Peak discharge and runoff coefficient

490 Gaume et al., (2009) used section S3 with a peak discharge of 1750 m^3/s and a cross-section area
491 of about 100 m^2. In doing so, they were using an apparent, field-based discharge instead of a
492 rainfall-based discharge (the difference between 1677 m^3/s in Table 2 and 1750 m^3/s is accounted
493 for through the roughness coefficient). Moreover, they missed the actual cross-section area in the
494 original data (López et al., 1964), which is 248 m^2 instead of about 100 m^2. Additionally, they
495 took a drainage area of 24 km^2 instead of 57 km^2. The consequence of an apparent discharge and
496 a misread drainage area was an specific (unit) peak discharge of 72 $m^3/s/km^2$, "considerably
497 higher than any of the other reported unit peak discharges in the inventory for similar watershed
498 areas and indeed higher than the world envelope curve" (ibidem). These erroneous figures spread
499 disbelief about the 1962 flash flood in Rubí, and led the authors to consider it a dubious outlier.
500 Apparent (field-based) discharge taken as rainfall-based discharge is the main misunderstanding.

501 The data review has shown that the 1962 flash flood deserves a proper, more careful
502 consideration. It will never be possible to accurately calculate the rainfall-based discharge, in
503 other words the water component of the flood. Following López et al. (1964), the peak flow went
504 from 320 (S1) and 350 (S2) in the main tributary to 635 (S3) and 658 m^3/s (S4) in the main stream
505 (Table 2), less than the 400—600 range and 700—800 m^3/s respectively given by Pardé (1964).
506 Moreover, our replication of the method while updating the sediment transport fundamentals
507 requires discharges of 370 (S1) and 391 m^3/s (S2) to hit the flooding marks in the tributary.

508 The unit discharge derived by López et al. is 14.5 $m^3/s/km^2$ in the main tributary (with our updated
509 calculations it is 16.5 $m^3/s/km^2$) and $\approx$ 11 — 8 $m^3/s/km^2$ in the main stream (Table 2). These are
510 not outliers at all. Indeed, a review of floods in the Mediterranean basins of Catalonia (Montalbán,
511 1994) stated the following envelope curve for all data:

512 $$Q\ (m^3/s/km^2) = 154 \cdot A\ (km^2)^{-0.621} \qquad (2)$$

513 where A is the basin area. Thus, the maximum unit discharges expected according to this formula
514 are $\approx$ 22 $m^3/s/km^2$ in S1-S2 of the main tributary and 12.5—10 $m^3/s/km^2$ in S3-S4 of Rubí for

areas of 57-82 km^2, respectively. Pardé (1964) gave very similar figures to those provided by Montalbán (1994), at least for the tributary (24—20 m^3/s/km^2). Our figures are not outliers either with respect to the recent collection of flash floods in Marchi et al. (2016).

More importantly, if the 1962 flash flood was really exceptional, the unit discharges should have touched the maximum, that is to say 22 m^3/s/km^2 in the main tributary, whereas the figure only reached 14.5 (López et al., 1964) or 16.5 m^3/s/km^2 according to us. This may suggest that the 1962 flood was not so extreme and its return period was less than 200 years. This may also suggest that the rainfall-based discharges in 1962 were significantly larger than both López et al. and our own estimate, given the limit provided by Montalban (1994): for example a maximum discharge of 497 m^3/s at S1, according to the envelope. In this case, with higher rainfall-based discharges, the need for torrential factors (suspension and bedload) in order to reach the target flooding marks would not be so important. However, at any rate, an apparent discharge as high as 1130 m^3/s in S1 (Table 2) does not make sense, regardless of a rainfall-based discharge of 320 m^3/s (Table 2), or 370 m^3/s (Table 3), or 400 m^3/s (Pardé,1964) or even 497 m^3/s (Montalban, 1994). In other words, the exact figure is not very important.

Thisbrings the discussion to the point of runoff coefficient. The accuracy of hydrological rainfall-runoff modelling in ephemeral streams is undermined by the transmission losses of the channel (Martín-Vide et al., 1999). Indeed, a rainfall-runoff model was calibrated in that paper with moderate floods (up to 100 m^3/s) in the main tributary catchment, which was gauged since that time. The results were SCS curve numbers in the range of 65-80 and transmission losses of 10-65%. In the major flood of 1962 and, furthermore, being the flow overloaded by sediment, it is impossible to know how much water and for how long was lost through the wide, flat, pervious channel bed.We can only reasonably compare total rainfall and runoff volume. Using the average of rainfall gauges (1) and (3) (Table 1) for the main tributary basin at S1, a constant discharge of 320 / 370 m^3/s lasting 2 hours would have conveyed some 55 / 63% of the rainfall volume (a runoff coefficient of 0.55 / 0.63). The same is true for the isohyets map (Fig. 7b). Compare this with a maximum runoff coefficient of 0.15 in six years of minor floods (Martín-Vide et al., 1999).

542 Compare this also with the SCS curve numbers mentioned above. For the 1962 Rubí event,
543 Lumbroso and Gaume (2012) tried an SCS curve number of 100 and a rainfall of 180 mm in 1
544 hour just to prove that the field-based discharge made little sense, even in conditions of too high
545 a curve number (for the mostly agricultural basin of 1962) and of too short a storm.

546 An important consequence is that, under torrential flows, the discharges inferred in the field
547 should be carefully examined in order not to mislead apparent and rainfall-based discharges. This
548 refers both for natural sections and gauging stations. This has been pointed out already by several
549 authors (Williams and Costa, 1988, Lumbroso and Gaume, 2012).

550 6.2. Sediment load

551 We are not claiming that the method used by López et al., replicated here, is perfect, or even fully
552 correct. It does not make sense for the flood to have carried 38% of bedload material out of the
553 total flood volume, as reported by them. Although not impossible, this impressive figure should
554 be cut back to 1.8—7.7% (Table 3), since Q_s/Q means the same sediment/water ratio, expressed
555 not in bulk but at peak conditions. These figures fall in the water flood domain (Costa, 1988) and
556 seem consistent with measurements for smaller floods: 0.7—1.2%, in bulk (Martín-Vide et al.
557 1999). As a result, 1962 flooding marks may be explained without resorting to hyperconcentrated
558 flow, let alone to debris flow. It is worth noting that 1.8—7.7% is for example significantly higher
559 than the corresponding values in Alpine water floods, for which the ratio is $Q_s/Q = 1.95 \cdot S_0^{1.5}$
560 (Rickenmann, 2012) (Q_s/Q includes pore volume). This formula would only yield 0.3—1.1% for
561 our case, that is to say 6-7 times less than in Table 3.

562 It seems, therefore, that the stream carries large amounts of sediment. There are some reasons in
563 support of this statement: *i*) a quite dense flow, called `mud´ for the sake of brevity, boosted by
564 plenty of fines available in the basin; *ii*) the sediment transport is not limited by supply, unlike in
565 many cases for mountain rivers (Rickenmann, 2012), because of the high availability of clasts,
566 significantly those in the very wide, flat channel, *iii*) the lack of an armour layer in the bed
567 promotes particle mobility, unlike perennial gravel-bed rivers (Reid and Laronne, 1995). This

568 feature is due to the ephemeral flow regime and, in particular, to the quick flow recession (Laronne
569 et al, 1994).

570 Moreover, the bed grain size D_m for the main tributary may not be very coarse in relation to its
571 very steep gradient S_0. A high ratio S_0/D_m means that any disturbance to the morphological
572 balance would have heavy consequences through large sediment loads (Leliavsky, 1955). This
573 parameter is almost the same as the excess shear θ / θ_c in Table 2, which is very high. Both
574 parameters point to high sediment loads in our case. In turn, the unit stream power, although high
575 (see Table 2), does not place this particular flood above the upper limits for flash floods in Europe
576 and the Mediterranean area (it has been exceeded in other documented flash floods, Marchi et al.,
577 2016). The unit stream power includes the ratio S_0/W (see caption to Table 2). A high width W
578 in our case contributes to the sediment load because of the unlimited supply of particles, but it is
579 in the denominator of the unit stream power. The parameters containing either S_0/D_m or S_0/W are
580 higher in the steep tributary than in the main river. Consequently, the tributary should have carried
581 more sediment and had a more torrential behaviour than the main river, as the calculation of
582 torrential depths has shown.

583 Finally, there is another phenomenon related to large sediment transport in steep streams that has
584 not been mentioned so far. A transient bed aggradation during the flood peak, probably linked to
585 bank scouring upstream, would reduce the actual flow area and therefore push torrential stages
586 up. It is true that the bed profile (Fig.9) turns milder around the junction, suggesting the possibility
587 of aggradation in the Rubí area, but no real data supports this suggestion, not even the pictures
588 (Fig. 5). Two points can be added: *i*) the large amount of sediment during the event may have
589 been transferred to the large Llobregat river, not far from Rubí (see Fig.2), which has a much
590 flatter gradient, *ii*) a slow incision is taking place since 1962 (Martín-Vide and Andreatta, 2009).

591 6.3. Torrential flow

592 There should be no doubt about the fact that the flooding marks were inexplicable in terms of
593 clear water flow. Nevertheless, in this respect the data clearly fall into two groups. The marks in
594 S1 and S2 on one side, located within the very steep tributary reach (3.24—2.95% slope) and with

595 no bridge failure upstream, agree with the torrential method. In short, the method enables a clear
596 water depth of 1.60 m to become a torrential depth of 2.60 m, due to the bedload driven by the
597 steep slope, together with a high wash load. The second group of data is made of cross-sections
598 S3 and S4 as well as cross-section A-A´ (Fig. 8). See its discussion in the next section.

599 The first depth increase from clear water to `mud´ flow (8—19% in Table 3, at S2-S1) could have
600 been approached using basic fluid mechanics. Assume that viscosity increases from 1 centipoise
601 (clear water) to 20 poise in concentrated mud while still behaving as a Newtonian fluid (Costa,
602 1988). This reduction of the Reynolds number moves the regime from fully turbulent to
603 transitional flow, raising the Darcy-Weisbach friction factor by 24% (on average), the Manning
604 roughness coefficient by 11% (idem) and therefore raising the depth by 7% at the most. Regarding
605 the influence of bedload in the second depth increase form `mud´ to torrential flow, the results of
606 Recking et al (2008), mostly based on flume experiments, would clearly underestimate our case.
607 The field setting and the denser flow that enhances bed mobility by increasing buoyancy are
608 thought to be reasons for the underestimation.

609 Flow velocities in floods are not much greater than 5 m/s, but typically in the range of 4—5 m/s
610 as a maximum, even for steep streams. A case study of the 1940 flood in Roussillon (France) has
611 provided real data about torrential flood velocities (Generalitat, 1990). The consequence of an
612 apparent discharge and a misread flow area led Gaume et al. (2009) to obtain an average flow
613 velocity of 17 m/s for our event, which they correctly rejected. In this sense, the velocities
614 resulting from the torrential method (Table 3) are more reasonable than both the velocities
615 calculated using apparent discharges ('virtual' in the heading, Table 2), and clear water velocities
616 (Table 3). Along the same lines, the Froude number in flash floods is generally below one
617 (subcritical flow). If the Froude number of a cross-section is found to be significantly greater than
618 one ($Fr > 1.3$) in a field estimation of discharge, then it is likely that the flow velocity is
619 overestimated (Lumbroso and Gaume, 2012). The Froude numbers (Table 3) are more reasonable
620 with the torrential magnitudes (depth and velocity) than with the clear water ones. The field-based

621 figures for the Froude number are Fr > 1.30 for three of the four cross-sections (data in Table 2).
622 This provides some support to the method, but not any validation.

623 6.4. The effect of bridges

624 An apparent discharge of thousands of m^3/s at A-A´ leaves no room for doubt about the role of
625 bridge blockage and failure, in this case. A blockage by a jam raises the level upstream so as to
626 raise the flood marks. Cross section S4 is located ≈ 0.3 km upstream of A-A´, which means it
627 should have shown the impact of the bridge at A-A´. Otherwise, it is difficult to explain why
628 cross-section S4 is so different from the rest of sections in the replicated method, or why the
629 method leaves the prediction so far away from the target. In other words, it is hard to see why the
630 apparent discharge climbs up to 3132 m^3/s (Table 2). Regarding S3, its moderate departure from
631 the method may be caused by a lesser backwater effect from the bridge located at A-A´, which is
632 farther downstream.

633 A sudden bridge failure produces a wave that travels downstream. The instantaneous release of a
634 height H in a channel of width B produces a peak flow Q equal to (Henderson, 1966):

635 $$Q\ (m^3/s) = \frac{8}{27}\cdot\sqrt{g}\cdot B \cdot H^{3/2} \qquad (3)$$

636 where g = 9,81 m/s^2. For B=50 m (real width) and H=7.7 m (less than the depth at A-A´), Q≈1000
637 m^3/s. The estimate of some 1000—1200 m^3/s, due to bridge collapses along several kilometres
638 (Pardé, 1964) may be quite correct. Obviously, the passage of such a wave downstream (a surge)
639 lifts the flood marks above those attained by a flow without failed bridges. Given the location
640 along the stream of the bridges that failed, on one side, and the surveyed cross-sections, on the
641 other side (Fig.9), group S3-S4 was affected by surges, while group S1-S2 was not. The latter
642 group was not even affected by the jam observed at the bridge in Fig.3a (x=13.2 km), which
643 withstood the flood, because cross-sections S1 and S2 are 3 km and 4 km upstream from it
644 (compare to the shorter distance from S3-S4 to A-A´ in Fig.9). Bridge failures upstream may have
645 a greater or lesser impact on the marks at S3-S4 in comparison to the backwater produced by the
646 blockage at the bridge at A-A´. Will never know which effect was dominant. In conclusion, the

torrential method replicated here should not be applied just upstream of a bridge that got jammed, nor anywhere downstream of a bridge that failed. The same should be said of any prediction of torrential flow (for example, based on advanced fluid mechanics) that assumes steady uniform flow.

In conclusion, the extreme stages in Rubí during the 1962 flash flood, like the S3, S4 andA-A´ cross-sections, can be explained by the effect of the bridges. In addition, the surges caused by bridge failures may have counteracted the possible bed aggradation through strong dragging on the bed.

6.5. Draft of an uncertainty analysis

The accuracy in the survey of flooding marks can be a concern, especially because the torrential depths were relatively small (2.0—4.9 m). Geomorphic effects such as aggradation linked to bank erosion (more likely) or scouring (less likely) are a second source of inaccuracy. The point is whether the cross-sectional geometry surveyed after the flood is different from the one existing at the time of the peak flow (Amponsah et al., 2016). In comparison to flooding marks and geomorphic effects, other inacuracies involved in the application of Manning formula are deemed negligible. The roughness coefficient of a very wide, flat bed that supplies particles with no limit should not depart much from the roughness due to its D_{50} grain size. The bed slope should not depart much from the alluvial fan gradient in the flow direction.

Following Amponsah et al (2016), the field-based discharge in Table 2 would be −34% in case of major aggradation (amounting to 20% of the depth) and −21% in case of small to moderate aggradation (amounting to 12% of depth). In addition, both results assume a ± 5% error in the survey of the flooding marks (then errors of 10—25 cm). The positive signs in case of scouring, i.e. +34% and +12%, are not sensible. Therefore, despite geomorphic effects and errors in surveying marks, the apparent discharge of 1130 m^3/s at S1 (Table 2), for example, continues not to make sense, despite being reduced by 34% to 746 m^3/s or by 21% to 893 m^3/s and the same for S2… S4. These field-based discharges are still twice as much as the rainfall-based estimates. They

673 still would produce outliers in terms of unit discharge (eq. 2) and roughness coefficients higher
674 than one.

675 6.6 Closure

676 The Rubí flash flood of 1962 is not an outlier in terms of total rainfall, return period of
677 precipitation, discharge, discharge per unit basin area, unit stream power, flow velocity or Froude
678 number, all kinematic magnitudes. If there is anything extraordinary about this flood, it is that it
679 reached very high stages at locations away of bridges, probably by transporting large amounts of
680 sediment. But it can be said that this flood was extraordinary due to the number of people who
681 died, and this is the main lesson for us to learn.

682 7. Conclusion

683 An organized convective system crossed Catalonia from southwest to northeast between the
684 afternoon of 25 September and the morning of 26 September 1962. It was not an isolated
685 disturbance. A cold front crossed the Iberian Peninsula from 24 to 26 September. On 25
686 September, it seems that a warm advection from the south increased instability in low levels to
687 the east of the Peninsula. An anticyclone to the northwest of the Mediterranean Sea had favoured
688 high temperatures in Catalonia in the days prior to the event. The convective energy and instability
689 in low levels was probably triggered by a mesoscale low formation at sea.

690 With all these factors, 200 mm of rainfall was recorded in the Rubí basin in less than 3 hours. The
691 rainfall rate surpassed 6 mm/min. The convective system must have stayed stationary over a large
692 region, including the Rubí basin. Other observatories recorded higher rainfall, but most damages
693 and casualties were reported there, because it was most vulnerable area (people had been pushed
694 to live in risky conditions). In addition, the water stages were unusually high.

695 The flash flood on the evening and night of 25 September 1962 in the Rubí stream, the worst
696 flood ever to take place in the country, left 815 people dead or missing. Figures 3 and 5 show the
697 scope of the devastation. In the upper reach, the shifting course of the main tributary on its flat
698 alluvial fan, where people had built their homes, was lethal. In the flood area houses and factories

were torn down in the two cities through which the stream passes. The economic damage was incalculable, to the point that the incoming migration to the region turned into an outgoing flux after the flood. Therefore, the1962 flash flood deserves to be recognised on an international scale, despite certain misunderstandings.

The marks left by the flood, carefully surveyed shortly after, cannot be explained by a clear water flow. Indeed, discharges calculated with these marks under the assumption of clear water flow, called apparent discharges, are 2 to 4 times larger than the approximate rainfall-based water discharges. For the flow to explain the high marks left by the flood, it is necessary to take into account the transport of both fine and coarse sediment and the effect of bridges.

A method relating to the influence of the wash load and bedload on the flow, already used in 1964, is updated in this paper, giving reasonable results to explain the flood. It allows us to reach the target of high torrential depths, while at the same time torrential velocities remain under 4—5 m/s. The method is able to distinguish cross-sections in which data was affected by bridge blockages downstream (through backwater) and by bridge failures upstream (through surges).

Acknowledgements

This paper was written under the framework of the Spanish projects HOPE (CGL2014-52571-R) and CGL2015-71291-P.

References

Amengual, A., Romero, R., Gómez, M., Martín, A., Alonso, S., 2007. A hydrometeorological modeling study of a flash flood event over Catalonia, Spain, Journal of Hydrometeorology, 8, 282-303.

Amponsah, W., Marchi, L., Zoccatelli, D., Boni, G., Cavalli, M., Comiti, F., Crema, S., Lucía, A., Marra, F., Borga, M. 2016. Hydrometeorological characterization of a flash flood associated with major geomorphic effects: assessment of peak discharge uncertainties and analysis of the runoff response. Journal of Hydrometeorology, JHM-D-16-0081.1.

Ashida, K., Michiue, M., 1972. Study on hydraulic resistance and bed load transport rate in alluvial streams. Trans.Japan Soc. Civ. Eng., 206, pp.59-69.

Aulet, J., Cabezas, S., Clua, F., Fernández, A., Ferrer, M., Frigola, E., Llasat, M.C., Màrquez, M., Masó, A., Masó, O., Mauri, F., Plans, L., Pont, F., Puig, LL. 2012. The 1962 flood, 50 years later (in Catalan). Ed. Amfora, Fund. Torre del Palau, Els Llibres de Terrassa, Ajunt.Terrassa.

729 Chien, N., Wan, Z., 1999. Mechanics of Sediment Transport. A.S.C.E., Reston.

730 Coll Ortega, J.M., 1963. Catastrophic floods in the Besòs and Llobregat rivers focusing the
731 torrential aspects (in Spanish). Montes 110, 111-123, march-april 1963.

732 Conesa-García, C., 1995. Torrential flow frequency and morphological adjustments of ephemeral
733 channel in south-east Spain, in: River Geomorphology, ed. Hickin, E., John Wiley & Sons,
734 Chichester, 169–192.

735 Costa J.E., 1988: Rheologic, geomorphic, and sedimentologic differentiation of water floods,
736 hyperconcentrated flows, and debris flows. In: Flood Geomorphology, Ed. by V.R. Baker, R.C.
737 Kochel, P.C. Patton; J. Wiley & Sons, New York, pp. 113-122.

738 Coussot, Ph., 1997. Mudflow Rheology and Dynamics. A.A.Balkema, Rotterdam.

739 García, C. and Martín-Vide, J.P. 2001, Grain-size distribution of a mobile bed in an ephemeral
740 gravel-bed stream. Application to a selected reach in Les Arenes stream (in Spanish). Acta
741 Geologica Hispanica, 36, 1-2, p.137-147

742 García Nájera, J.M. (1962) (1st ed. 1943). Principles of torrential hydraulics and its application
743 to torrent training (in Spanish) Agriculture Ministry. IFIE, Madrid.

744 Gaume, E.; Bain,V.; Bernardara, P.; Newinger, O.; Barbuc, M.; Bateman, A.; Blaškovicova, L.;
745 Blöschl, G.; Borga, M; Dumitrescu, A.; Daliakopoulos, I.; Garcia, J.; Irimescu, A.; Kohnova, S.;
746 Koutroulis, A.; Marchi, L.; Matreata, S.; Medina, V.; Preciso, E.; Sempere-Torres, D.; Stancalie,
747 G.; Szolgay, J.; Tsanis, I.; Velasco, D.; Viglione, A. (2009). A compilation of data on European
748 flash floods. Journal of Hydrology 367 pp.70–78.

749 Generalitat de Catalunya (1990). The 1940 flood (`L'aiguat del 40´) (in Catalan).

750 Gibergans-Bàguena, J. and Llasat, M.C., 2007, Improvement of the analog forecasting method by
751 using local thermodynamic data. Application to autumn precipitation in Catalonia. Atmospheric
752 Research, 86, 173-193.

753 Henderson, F.M. (1966). Open channel flow. McMillan publisher.

754 Laronne, J.B., Reid, I., Yitshack, Y., Frostick, L.E. 1994. The non-layering of gravel streambeds
755 under ephemeral flood regimes. Journal of Hydrology, 159, 353-363.

756 Leliavsky, S. 1955. An Introduction to Fluvial Hydraulics. Constable, London.

757 Llasat, M.C., 1987. Events of heavy rain in Catalonia: genesis, evolution and contributing factors
758 (in Spansih). Publ. Univ. de Barcelona, nº40, 543 pp. Barcelona.

759 Llasat, M.C., 2001. An objective classification of rainfall events on the basis of their convective
760 features. Application to rainfall intensity in the north-east of Spain. International Journal of
761 Climatology, Vol. 21, nº11, 1385-1400

762 Llasat, M.C., T. Rigo, M. Barriendos, 2003, The 'Montserrat-2000'flash-flood event: a
763 comparison with the floods that have occurred in the northeastern Iberian Peninsula since the 14th
764 Century, International Journal of Climatology, 23, 4, 453-469.

765 Llasat, M.C., Martín, F. and Barrera, A., 2007. From the concept of "Kaltlufttropfen" (cold air
766 pool) to the cut-off low. The case of September 1971 in Spain as an example of their role in heavy
767 rainfalls, Meteorology and Atmospheric Physics, 96, 43-60.

768 Llasat, M.C., 2009. Chapter 18: Storms and floods, in The Physical Geography of the
769 Mediterranean basin. Jamie Woodward (ed). Oxford University Press, pp. 504-531.

770 Llasat, M. C., Llasat-Botija, M., Petrucci, O., Pasqua, A.A., Rosselló, J., Vinet, F., Boissier, L.,
771 2013. Towards a database on societal impact of Mediterranean floods in the framework of the
772 HYMEX project. Nat. Hazards Earth Syst. Sci., 13, 1–14.

773 Llasat, M.C., Marcos, R., Llasat-Botija, M., Gilabert, J., Turco, M., Quintana, P., 2014. Flash
774 flood evolution in North-Western Mediterranean. Atmospheric Research 149, 230–243.

775 Llasat, M.C., R. Marcos, M. Turco, J. Gilabert, M. Llasat-Botija, 2016. Flash floods trends versus
776 convective precipitation in a Mediterranean region. Journal of Hydrology, 541, 24-37,
777 http://dx.doi.org/10.1016/j.jhydrol.2016.05.040 0022-1694

778 López Bustos, A.; Coll Ortega, J.M.; Llansó de Viñals, J.M.; Espinosa Franco, R. (1964).
779 Summary and conclusions of the Vallés flood of 1962 (in Spanish). Instituto Hidrología, Madrid.

780 Lumbroso, D., Gaume, E. (2012). Reducing the uncertainty in indirect estimates of extreme flash
781 flood discharges. J. Hydrol., 414-415, 16-30.

782 Marchi. L., Cavalli, C., Amponsah, W., Borga, M., Crema, S. (2016). Upper limits of flash flood
783 stream power in Europe. Geomorphology, 272, 68-77.

784 Martín León, F., 2004, Floods of 25 September 1962 in Catalonia (in Spanish). Rev. Aficio Meteo
785 (http://www.tiempo.com/ram/1598/las-inundaciones-de-catalua-del-25-de-septiembre-de1962/).

786 Martín-Vide, J.P., Niñerola, D., Bateman, A., Navarro, A., Velasco, E. (1999). Runoff and
787 sediment transport in a torrential ephemeral stream of the Mediterranean coast. Journal of
788 Hydrology, vol.225/3-4, pp.118-129.

789 Martín-Vide, J.P. (2006), River Engineering (in Spanish), Ed.UPC, Barcelona.

790 Martín-Vide, J.P., Andreatta, A. (2009). Channel Degradation and Slope Adjustment in Steep
791 Streams Controlled through Bed Sills. Earth Surface Processes and Landforms, 34, 38-47.

792 Meunier, M. 1991. Elements of torrential hydraulics (in French). Cemagref, Grenoble.

793 Mintegui, J.A. Homage to dr. J.M. García Nájera (in Spanish). Congreso Forestal Español, 1993.

794 Montalbán, F. (1994) Recommendations for maximum flood estimation methods (in Catalan).
795 Junta d'Aigües. Generalitat de Catalunya.

796 Pardé, M. 1964. Fluvial regimes of the Iberian peninsula (in French). Géocarrefour, 39, 3, pp.129-
797 182.

798 Public Works Department (1999). Maximum daily raifall in Spain (in Spansih). Ministerio de
799 Fomento, Madrid.

800 Puigcerver, M., Alonso, S., Lorente, J., Llasat, M.C., Redaño, A., Burgeño, A., Vilar, E., 1986.
801 Preliminary aspects on rainfall rates in the north east of Spain. Theor.Appl.Climatol. 37, 97-109.

802 Ramis, C., Llasat, M.C., Genovés, A., Jansà, A., 1994. The October-87 floods in Catalonia.
803 Synoptic and mesoscale mechanisms. Meteorological Applications 1, 337-350.

804 Ramos, A.M., Trigo, R.M., Liberato, M. L. R., Tomé, R., 2015. Daily Precipitation Extreme
805 Events in the Iberian Peninsula and Its Association with Atmospheric Rivers. J. of
806 Hydrometeorology, 16, 579-597. DOI: http://dx.doi.org/10.1175/JHM-D-14-0103.1.

807 Recking, A, Frey P., Paquier, A., Belleudy, P. and Champagne, J.Y. , 2008. Feedback between
808 bed load transport and flow resistance in gravel and cobble bed rivers. Water Resources Research
809 44, W05412, doi:10.1029/2007WR006219.

810 Reid, I., Laronne, J.B, 1995. Bedload sediment transport in an ephemeral stream and a comparison
811 with seasonal and perennial counterparts. Water Resources Research,31(3),773-781.

812 Rickenmann, D. 1991, Hyperconcentrated flow and sediment transport at steep slopes. Journal of
813 Hydraulic Engineering ASCE, vol.117, pp.1419-1439.

814 Rickenmann, D. 2012, Alluvial Steep Channels: Flow Resistance, Bedload Transport Prediction
815 and Transition to Debris Flows. Chapter 28 of Gravel-bed Rivers: Processes, Tools,
816 Environments, Ed. by M. Church, P. M. Biron and A. G. Roy. John Wiley & Sons, Ltd.

817 Rigo, T. and M.C. Llasat, 2005: Radar analysis of the life cycle of mesoscale convective systems
818 during the 10 June 2000 event. Natural Hazards and Earth System Sciences, 5, 1-12.

819 Song, T, Chiew, Y.M., Chin, C.O., 1988. Effects of bed-load movement on flow friction factor.
820 Journal of Hydraulic Engineering ASCE, 124, 2, 165.

821 Takahashi, T., 2007. Debris Flow. Mechanics, Prediction and Countermeasures. CRC Press.

822 Trapero, L., Bech, J., Duffourg, F., Esteban, P., Lorente, J., 2013. Mesoscale numerical analysis
823 of the historical November 1982 heavy precipitation event over Andorra (Eastern Pyrenees). Nat.
824 Hazards Earth Syst. Sci. 13, 2969-2990.

825 Valls i Vila, J., 2012. The 1962 flood, a catastrophe that shook the invertebrate Terrassa of
826 Francoism (in Catalan). Col. 50 anys riada Terrassa, Ed. Ajunt. Terrassa.

827 Wan, Z.and Wang, Z., 1994. Hyperconcentrated flow. A.A.Balkema

828 Williams, G.P. and Costa, J.E., 1988. Geomorphic measurements after a flood. In: Flood
829 Geomorphology, op.cit., pp.65-77.